



Natural Resources  
Canada

Ressources naturelles  
Canada



# **Characteristics of glacial Lake McConnell clay, Great Slave Lowland, Northwest Territories**

*A.A. Aden, S.A. Wolfe, J.B. Percival, and A. Grenier*

**Geological Survey of Canada  
Current Research 2015-7**

**2015**



---

**Geological Survey of Canada**  
**Current Research 2015-7**

---



**Characteristics of glacial Lake McConnell clay,  
Great Slave Lowland, Northwest Territories**

*A.A. Aden, S.A. Wolfe, J.B. Percival, and A. Grenier*

**2015**

© Her Majesty the Queen in Right of Canada, as represented by the Minister of Natural Resources Canada, 2015

ISSN 1701-4387

Catalogue No. M44-2015/7E-PDF

ISBN 978-0-660-02828-6

doi:10.4095/296860

A copy of this publication is also available for reference in depository libraries across Canada through access to the Depository Services Program's Web site at <http://dsp-psd.pwgsc.gc.ca>

This publication is available for free download through GEOSCAN  
<http://geoscan.nrcan.gc.ca>

#### **Recommended citation**

Aden, A.A., Wolfe, S.A., Percival, J.B., and Grenier, A., 2015. Characteristics of glacial Lake McConnell clay, Great Slave Lowland, Northwest Territories; Geological Survey of Canada, Current Research 2015-7, 12 p. doi:10.4095/296860

#### **Critical review**

*P. Morse*

#### **Authors**

**A.A. Aden** ([ayana.aden@mail.utoronto.ca](mailto:ayana.aden@mail.utoronto.ca))

*Department of Geography and Planning*

*University of Toronto*

*St. George Campus*

*Sidney Smith Hall*

*100 St. George Street*

*Toronto, Ontario*

*M5S 3G3*

**J.B. Percival** ([Jeanne.Percival@canada.ca](mailto:Jeanne.Percival@canada.ca))

**A. Grenier** ([Alain.Grenier@canada.ca](mailto:Alain.Grenier@canada.ca))

*Geological Survey of Canada*

*601 Booth Street*

*Ottawa, Ontario*

*K1A 0E8*

**S.A. Wolfe** ([Stephen.Wolfe@canada.ca](mailto:Stephen.Wolfe@canada.ca))

*Geological Survey of Canada*

*601 Booth Street*

*Ottawa, Ontario*

*K1A 0E8*

**Also at:**

*Carleton University*

*Department of Geography and Environmental Studies*

*1125 Colonel By Drive*

*Ottawa, Ontario*

*K1S 5B6*

Correction date:

Information contained in this publication or product may be reproduced, in part or in whole, and by any means, for personal or public non-commercial purposes, without charge or further permission, unless otherwise specified.

You are asked to:

- exercise due diligence in ensuring the accuracy of the materials reproduced;
- indicate the complete title of the materials reproduced, and the name of the author organization; and
- indicate that the reproduction is a copy of an official work that is published by Natural Resources Canada (NRCan) and that the reproduction has not been produced in affiliation with, or with the endorsement of, NRCan.

Commercial reproduction and distribution is prohibited except with written permission from NRCan. For more information, contact NRCan at [nrcan.copyrightdroitdauteur.nrcan@canada.ca](mailto:nrcan.copyrightdroitdauteur.nrcan@canada.ca).

# Characteristics of glacial Lake McConnell clay, Great Slave Lowland, Northwest Territories

A.A. Aden, S.A. Wolfe, J.B. Percival, and A. Grenier

Aden, A.A., Wolfe, S.A., Percival, J.B., and Grenier, A., 2015. Characteristics of glacial Lake McConnell clay, Great Slave Lowland, Northwest Territories; Geological Survey of Canada, Current Research 2015-7, 12 p. doi:10.4095/296860

---

**Abstract:** Grain-size analysis from a drilling program 30 km west of Yellowknife defined three distinct sediment groups: a lowermost clay-rich unit (Group 1), a middle silt-rich unit (Group 2), and a sand-rich upper unit (Group 3). Physical properties and mineralogy were investigated for two fine-grained clay samples by the GSC Sedimentology Laboratory and X-ray Mineralogy Laboratory, respectively; sediment texture was determined by the authors. Both samples plot above the A-line of the Casagrande plasticity chart, indicating they are clays with intermediate to high plasticity, and classified by Atterberg limit analysis as inactive. The majority of nonclay minerals in the clay-size fraction are quartz; and the remaining clay minerals are primarily detrital mica, chlorite, and kaolinite. Minor to trace amounts of mixed-layer clay minerals (most likely illite-smectite) are noted in the clay-size fractions, whereas only trace amounts are observed in other group samples. These analyses confirm that the two samples fall within Group 1, and are glaciolacustrine, originating from glacial Lake McConnell (ca. 13.0–9.5 ka), and derived primarily from local granitic bedrock, with perhaps some weathering or allogenic contribution, resulting in traces of mixed-layer clay minerals. Scanning electron microscope analysis revealed subrounded to subangular silt-size grains of detrital origin, randomly distributed in a clay matrix; with possible evidence of minor compaction within the soil. Coarser grain size, higher quartz content, and only trace mixed-layer clay minerals suggest that Group 2 and 3 sediments originate from reworking and redeposition of Group 1 sediments within lacustrine or alluvial settings. High ground-ice contents imply these sediments are prone to instability if thawed.

**Résumé :** L'analyse granulométrique d'échantillons d'un programme de forage réalisé à 30 km à l'ouest de Yellowknife a permis de définir trois groupes de sédiments distincts : une unité basale riche en argiles (groupe 1), une unité intermédiaire riche en silt (groupe 2) et une unité supérieure riche en sable (groupe 3). L'étude des propriétés physiques et de la minéralogie de deux échantillons de sédiments argileux à grain fin a été réalisée au Laboratoire de sédimentologie et au Laboratoire de minéralogie par diffraction des rayons X de la CGC, respectivement; la texture sédimentaire a été déterminée par les auteurs. Les deux échantillons se situent au-dessus de la ligne A du diagramme de plasticité de Casagrande, ce qui indique qu'il s'agit d'argiles à plasticité intermédiaire à élevée, et sont classés comme inactifs selon l'analyse des limites d'Atterberg. La majorité des minéraux non argileux dans la fraction granulométrique des argiles est constituée de quartz; les minéraux argileux restants sont principalement composés de mica, de chlorite et de kaolinite détritiques. Des minéraux argileux interstratifiés (vraisemblablement d'illite-smectite) ont été relevés en quantités mineures ou en traces dans la fraction granulométrique des argiles, tandis que seules des traces sont observées dans les autres échantillons. Ces analyses confirment que les deux échantillons se situent dans le groupe 1 et sont glaciolacustres, c'est-à-dire qu'ils ont leur source dans le Lac glaciaire McConnell (env. 13,0–9,5 ka) et qu'ils dérivent principalement du socle granitique local, avec une possible part d'altération météorique ou de contribution allogène pour expliquer la présence de minéraux argileux interstratifiés en traces. Une analyse au microscope électronique à balayage a révélé l'existence de grains de silt subarrondis à subanguleux d'origine détritique, distribués de manière aléatoire dans une matrice argileuse, ainsi qu'une preuve possible de compaction mineure dans le sol. Le grain plus grossier, la concentration plus élevée de quartz et la présence de minéraux argileux interstratifiés qu'en traces seulement donnent à penser que les sédiments des groupes 2 et 3 sont issus du remaniement et de la résédimentation des sédiments du groupe 1 dans des cadres lacustres ou alluviaux. Les fortes teneurs en glace de sol signifient que ces sédiments sont susceptibles d'être instables s'il y a fonte de la glace.

## INTRODUCTION

Permafrost, defined as perennially frozen ground remaining at or below 0°C for two or more years, underlies approximately a fifth of the world's surface and nearly half of Canada (Burn and Smith, 1993). Development of Canada's northern regions involves increasing infrastructure construction (e.g. buildings, roads, power supplies) under a range of permafrost conditions. In discontinuous permafrost terrain, construction and remediation of infrastructure can be particularly challenging, given highly variable conditions over relatively short distances and the warm thermal state of permafrost. Added to these already challenging conditions is the fact that mean annual air temperatures in northwestern Canada have increased by more than 1.5°C during the latter half of the last century (Maxwell, 1997) and that such warming trends in northern high latitudes are expected to continue during this century (Burn et al., 2004; Arctic Climate Impact Assessment, 2005). Within this context, the importance of studies assessing permafrost-affected terrain cannot be understated.

A typical example of road infrastructure traversing discontinuous permafrost and unstable, ice-rich terrain is Northwest Territories Highway 3. This corridor extends from the Mackenzie River near Fort Providence along the western and northern shores of Great Slave Lake, to Yellowknife (Fig. 1 inset). It is a critical transportation highway that supplies local communities and resource industries. Between Behchoko and Yellowknife, the highway extends across the extensive discontinuous zone of permafrost and the high boreal ecoregion of the Great Slave Lowland. This area contains fine-grained sediments known to be ice-rich (Stevens et al., 2012a, b). The objective of this study is to characterize the clay sediments that underlie this discontinuous

permafrost region. Herein, the authors analyze the physical, mineralogical, and sediment texture of two selected clay samples obtained as part of a larger investigation of permafrost conditions and occurrence of ice-rich terrain in the region. These clay samples were derived from glacial Lake McConnell (ca. 13.0–9.5 ka), a large proglacial lake that covered much of northwestern Canada (Wolfe et al., 2011; Percival et al., 2013) and from the subsequent (ancestral) Great Slave Lake that replaced it.

## MATERIALS AND METHODS

Samples were collected as part of a drilling program in the Boundary Creek study area located 30 km west of Yellowknife in the Great Slave Lowland (Fig. 1, inset). Five boreholes were cored into permafrost using a Cold Regions Research and Engineering Laboratories frozen ground corer to depths between 4 m and 8 m along a 50 m transect south of Highway 3 (Fig. 1). Boreholes 2–5 were located on the 4 m high ridge, whereas borehole 1 was drilled into the low-lying bordering peatland (Wolfe et al., 2014). Core samples were retrieved, with samples measuring 7.6 cm in diameter and 10 m to 20 cm in length. Moisture content (per cent dry weight) was determined on subsamples from each interval. Remaining samples were bagged, labelled according to depth, and shipped to the GSC in Ottawa, where they were kept refrigerated.

Selected samples were submitted to the GSC Sedimentology Laboratory (Northern Canada Division) for physical property analyses including grain size and Atterberg limits (Girard et al., 2004). Complete grain-size analysis was determined on less than 90 µm sieved samples using a LECOTRAC LT-100 Particle Size Analyzer (LECO Corporation), whereas the liquid limit and plastic limit

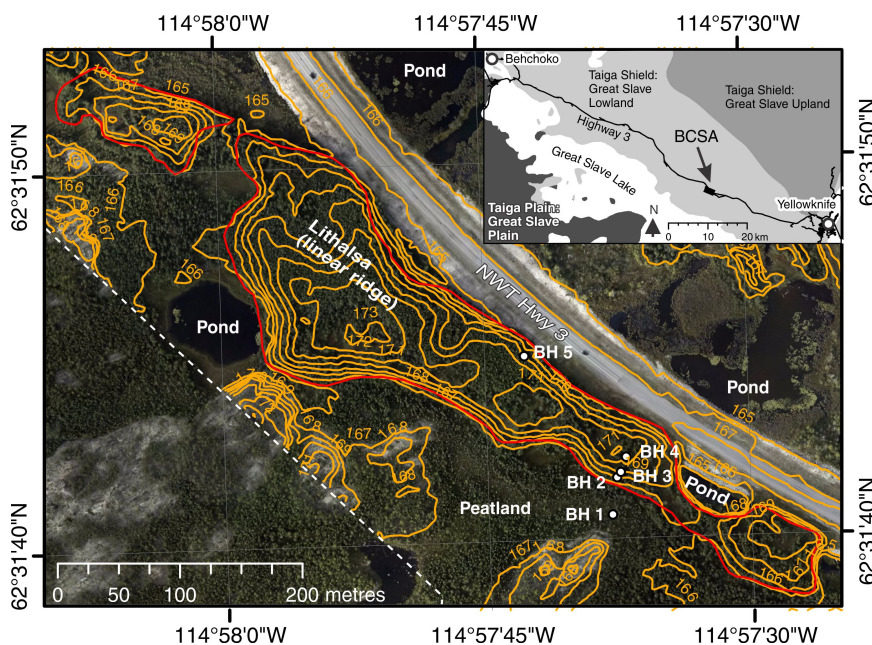


**Figure 1.** Boundary Creek study area (BCSA) west of Yellowknife (inset) and location of five boreholes within the peatland and ridge south of NWT Highway 3.

were determined using the Casagrande method. Mineralogy was determined using X-ray diffraction on both the less than 2 mm bulk and the less than 2  $\mu\text{m}$  clay-size fractions. Semiquantitative mineralogy was determined by XRD in the X-ray (Mineralogy) Laboratory of the GSC (Central Canada Division). The less than 2  $\mu\text{m}$  clay-size fraction was prepared using centrifugation (International Equipment Company centrifuge model UV PR-7000) of a suspension in distilled water (Percival et al., 2001). Following centrifugation, the remaining suspension was decanted and the clay-size fraction was freeze-dried. Bulk samples were micronized in isopropyl alcohol using a McCrone mill. Samples were subsequently air dried and back pressed into an aluminum holder to produce a randomly oriented specimen. For clay-size separates, 40 mg were suspended in distilled water and pipetted onto glass slides and air dried overnight to produce oriented mounts. X-ray patterns of the pressed powders and air-dried samples were recorded on a Bruker D8 Advance Powder Diffractometer equipped with a Lynx-Eye detector, Co K $\alpha$  radiation set at 40 kV and 40 mA. The clay-size samples were also X-rayed following saturation with ethylene glycol and heat treatment (550°C) for two hours to identify specific clay minerals.

Initial identification of minerals was made using EVA (Bruker AXS Inc.) software with comparison to reference mineral patterns using Powder Diffraction Files (PDF) of the International Centre for Diffraction Data (ICDD) and other available databases. Quantitative analysis was carried out using TOPAS (Bruker AXS Inc.), a PC-based program that performs Rietveld refinement (RR) of XRD spectra. This is based on a whole pattern-fitting algorithm. Quantitative analyses appear reasonable when minerals in the samples can be matched to the standards. The lower the goodness-of-fit (GoF) value, the closer the standards match the unknowns and the better the results (Percival et al., 2003).

Two samples were selected for additional detailed mineralogical and textural analysis to determine their origin. These samples were collected from Borehole 4 from depths of 710–723 cm (WDA12-97) and 741–758 cm (WDA12-99), respectively (Fig. 2). Physical-property analysis measured on these samples also included moisture content, grain size, and Atterberg limits, and mineralogy was determined as per other samples. In addition, sediment texture was examined using a scanning electron microscope (SEM) on polished thin sections.

The two selected samples were slowly impregnated using Petropoxy in a vacuum oven. The samples were then sent to Vancouver Petrographics to prepare polished thin sections for sediment texture and petrographic analysis. The sections were examined under a Zeiss EVO 50 series scanning electron microscope with extended pressure capability (up to 3000 Pascals). The SEM is equipped with a backscattered electron detector (BSD), Everhart-Thornley secondary electron detector (SE), variable pressure secondary electron detector (VPSE), and a cathodoluminescence detector (CL). The Oxford EDS (energy dispersive spectrometry) system

includes the X-MAX 150 silicon drift detector, INCA Energy 450 software and the AZtec Energy 2.2 microanalysis software. Operating conditions include a working distance of 8.5 mm, high voltage (EHT) set at 20 kV, with a probe current of 400 pA to 1 nA, and a filament current set to second peak. Image store resolution is 1024  $\times$  768 pixels, and saved as .tif files.

## RESULTS

Figure 3 identifies stratigraphic units, based on sediment textures, and indicates occurrence of ice lenses and moisture contents within the boreholes. The stratigraphy identifies three primary units, including clayey-silt and silty-sand units and an underlying unit of clay in all boreholes. Ice lenses are smaller and moisture contents, reflecting the volume of ground ice within the sediments, are typically below 50% in the upper 4 m in all boreholes. Ground-ice contents increase below this depth, and particularly within the lower clay unit.

The locations of samples WDA12-97 and WDA12-99 from the clay unit in Borehole 4 are denoted by red stars in Figure 3. The largest volumes of ice are observed within this fine-grained section, and four coarse (0.6–1.0 mm diameter), subangular to subrounded sand grains were found in this layer.

## Physical properties

### Grain-size analysis

Sediment textures and grain-size distributions of borehole samples are shown in Figures 4a and b, respectively. It is evident that there are three distinct sediment groupings:

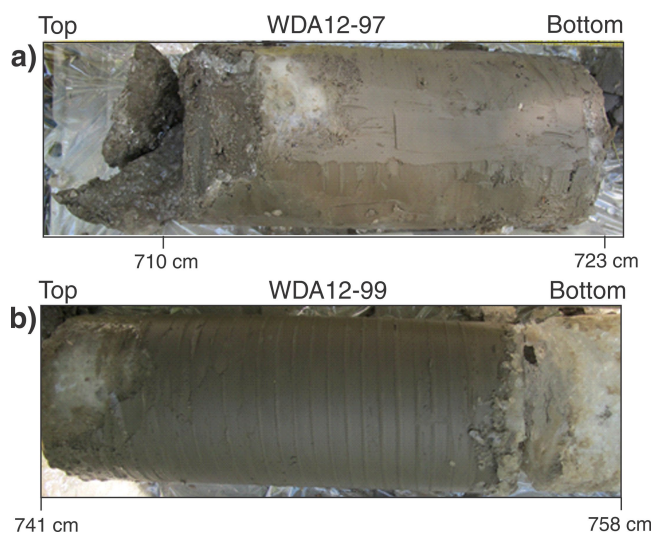


**Figure 2.** Core samples of **a)** WDA12-97 (710–723 cm; 2015-089) and **b)** WDA12-99 (741–758 cm; 2015-094) from Borehole 4. Note that parallel lines on soil sample are not laminations, but are indentations caused by the coring process.

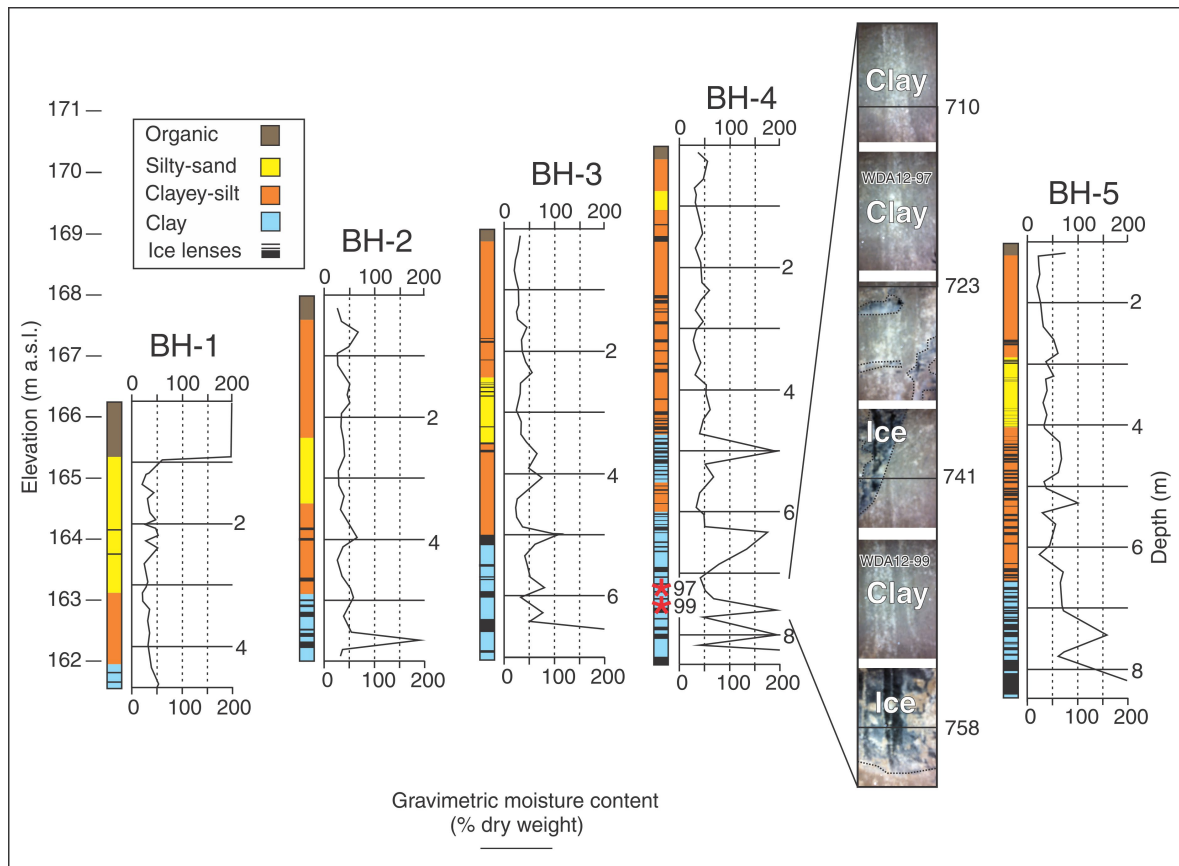


**Figure 3.** Borehole stratigraphy and gravimetric moisture contents (% dry weight). Location of samples WDA12-97 and WDA12-99 (red stars) and downhole borehole photographs from Borehole 4. Photograph by S. Wolfe. 2015-087

Group 1 represents the clay-rich lower unit in Figure 3, Group 2 is silt-rich and represents the intermediate and uppermost layers, and Group 3 is the sand-rich layer in all boreholes. Sample WDA12-97 and WDA12-99 both reside within the Group 1 clay-rich unit.

On average, Group 1 clays have a high percentage of clay (55.02%) and silt (43.44%) and a minimal component of sand (1.54%). The silt-rich Group 2 samples contain, on average, 67.71% silt, 21.81% clay, and 10.47% sand, whereas the sand-rich Group 3 has a lower percentage of clay (11.87%) and high percentages of silt (45.91%) and fine sand (42.22%). Sample WDA12-97 contains 60.44% clay, 39.20% silt, and 0.35% sand and WDA12-99 contains 56.03% clay, 43.70% silt, and 0.27% sand.

### Atterberg limits

Figure 4c and 4d show Atterberg limits of the analyzed samples. Most lie above the ‘A-line’ (Fig. 4c), which is a line separating clays from silts and organic materials from inorganic materials (Holtz and Kovacs, 1981). The samples also lie largely parallel to the A-line, and range between CL (intermediate plasticity) and CH (high plasticity). Figure 4c

further indicates that Group 1 sediments have higher liquid limits and plastic limits than Group 2 and Group 3 sediments, and are typically classified as clays of high plasticity. Notably, all groups are classified as clay, even though their sediment textures may indicate that they are typically coarser than clay. This attests to the significant influence that the clay-sized particles have on affecting the sediment properties. Figure 4d further illustrates that the Group 1 sediments, and both WDA samples, are of high plasticity and are classified as ‘inactive’. The WDA samples both have some of the highest clay contents. Samples WDA12-97 and WDA12-99 have liquid limits of 59.6% and 58.1%, plastic limits of 26.7% and 26.2%, and plasticity indices of 32.9 and 31.9, respectively.

### Moisture content and bulk density

Moisture contents and bulk density measurements of soil are summarized in Table 1. Moisture contents were 41.02% and 36.10% for WDA12-97 and WDA12-99, respectively. Respective average moisture contents for Groups 1, 2, and 3 are 84.27%, 37.09%, and 37.48%. Frozen bulk-density values for WDA12-97 and WDA12-99 were 1.83 g/cm<sup>3</sup> and 1.84 g/cm<sup>3</sup>, respectively; there is minimal variation



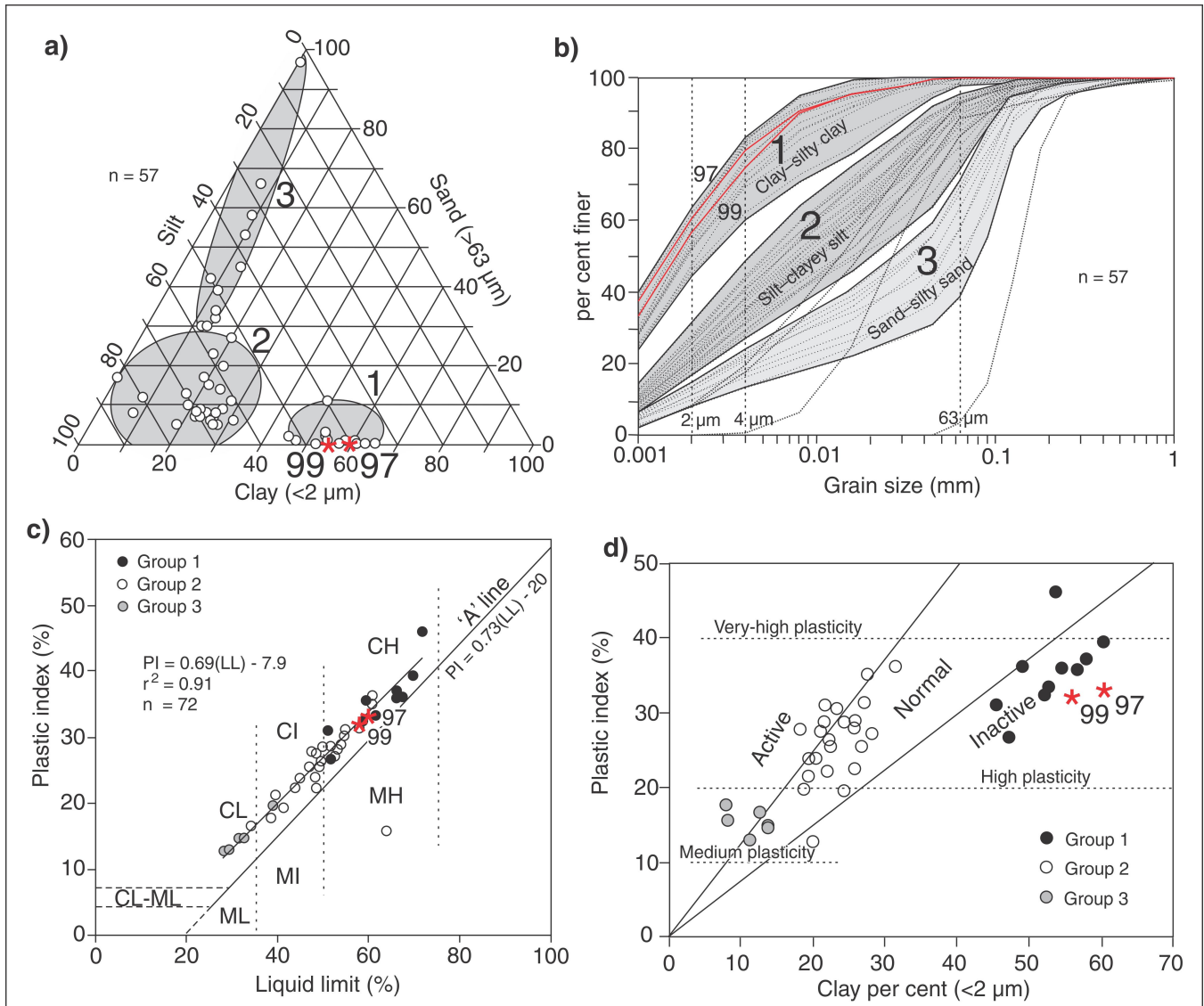


**Figure 4.** Grain-size and Atterberg limit results showing Group 1, Group 2, and Group 3 sediment classifications and results from samples WDA12-97 and WDA12-99 (red stars). **a)** Textural characteristics. **b)** Grain-size distributions. **c)** Plasticity based on Atterberg limits depicting Group 1, Group 2, and Group 3 sediment textures (CH = high-plasticity clay, CI = intermediate-plasticity clay, CL = low-plasticity clay, MH = high-plasticity silt, MI = intermediate-plasticity silt, ML = low-plasticity silt, PI = plastic index). **d)** Activity diagram for Group 1, Group 2, and Group 3 sediments.

in bulk density values for all samples throughout all three groups (mean = 1.53 g/cm<sup>3</sup>, 1.67 g/cm<sup>3</sup>, and 1.83 g/cm<sup>3</sup>, respectively).

## Mineralogy

Quantitative XRD analysis of the bulk (<2 mm) fraction is given in Table 2. Samples contain abundant quartz, plagioclase feldspar, and mica (variety muscovite) with average amounts of nonclay minerals for Groups 1, 2, and 3 as 77.2%, 81.6%, and 87.7%, respectively (Table 2). As grain size increases among the sediment groups, the proportion of nonclay minerals also increases, as reflected by the increase

in quartz and plagioclase feldspar. Samples WDA12-97 and WDA12-99 have nonclay mineral contents of 64% and 66%, respectively. Both samples have a lower nonclay mineral content, and hence higher clay mineral content, than other Group 1 sediments, reflecting the very fine-grained nature of these two samples.

Quantitative mineralogy of the less than 2 μm clay fraction of the samples is summarized in Table 3. Samples WDA12-97 and WDA12-99 are composed of abundant quartz, plagioclase feldspar, and muscovite and minor to trace mixed-layer clay minerals. The presence of the mixed-layer clay minerals provides some issues with quantitative analysis as there are no matching structure files available.

**Table 1.** Moisture content (%) and frozen bulk-density (g/cm<sup>3</sup>) values for samples WDA12-97 and WDA12-99 and for all Group 1, Group 2, and Group 3 samples.

Group	Sample ID	Dry-weight moisture content (%)	Frozen bulk-density (g/cm <sup>3</sup> )
	WDA12-97	41.02	1.83
	WDA12-99	36.10	1.84
Group 1 (n = 9)	Min.	32.15	1.21
	Max.	304.70	1.76
	Average	84.27	1.53
	SD	81.41	0.19
	Median	58.55	1.59
Group 2 (n = 24)	Min.	21.69	1.43
	Max.	66.70	2.12
	Average	37.09	1.67
	SD	11.53	0.16
	Median	35.58	1.63
Group 3 (n = 8)	Min.	28.27	1.52
	Max.	52.63	2.05
	Average	37.53	1.83
	SD	8.42	0.24
	Median	36.33	1.90

**Table 2.** Quantitative XRD analysis (wt %) of bulk (<2 mm) samples WDA12-97 and WDA12-99 and for all Group 1, Group 2, and Group 3 samples. The proportions of nonclay (Qtz+Pl+Kfs+Amp) and clay minerals (Ms+Kln+Chl) are shown for comparison. Qtz = quartz, Pl = plagioclase feldspar, Kfs = potassium feldspar, Amp = amphibole, Ms = muscovite, Kln = kaolinite, Chl = chlorite

Group	Sample ID	Qtz	Pl	Kfs	Amp	Ms	Kln	Chl	Nonclay	Clay
	WDA12-97	47	24	3	4	10	2	10	64	36
	WDA12-99	50	26	3	4	9	1	7	66	34
Group 1 (n = 13)	Min.	41	21	3	3	7	2	7	74	17
	Max.	55	26	4	5	15	3	11	83	26
	Average	46.3	23.5	3.3	4.1	10.8	2.3	9.7	77.2	22.8
	SD	4.27	1.45	0.45	0.67	2.29	0.49	1.37	2.89	2.89
	Median	45	23.5	3	4	11	2	10	76	24
Group 2 (n = 26)	Min.	51	19	2	2	7	1	6	78	14
	Max.	63	21	3	4	12	2	9	86	22
	Average	55.9	20.0	2.6	3.1	8.8	1.8	7.9	81.6	18.4
	SD	2.85	0.71	0.50	0.42	1.60	0.42	0.91	2.15	2.15
	Median	56	20	3	3	8	2	8	81	19
Group 3 (n = 9)	Min.	60	16	2	1	5	1	4	84	10
	Max.	66	22	2	3	7	3	8	90	16
	Average	63.4	20.1	2	2.2	5.7	1.3	5.3	87.7	12.3
	SD	2.01	1.66	0.00	0.79	0.67	0.67	1.34	2.11	2.11
	Median	63.5	20.5	2	2	6	1	5.5	87.5	12.5

**Table 3.** Semiquantitative XRD analysis (wt %) of the clay-size samples WDA12-97 and WDA12-99 and all Group 1, Group 2, and Group 3 samples. The proportions of nonclay (Qtz+Pl+Kfs+Amp) and clay minerals (Ms+Kln+Chl) are shown for comparison. Qtz = quartz, Pl = plagioclase feldspar, Kfs = potassium feldspar, Amp = amphibole, Ms = muscovite, Kln = kaolinite, Chl = chlorite, ML = mixed-layer clay, m = minor, tr = trace

Group	Sample ID	Qtz	Pl	Kfs	Amp	Ms	Kln	Chl	ML	Nonclay	Clay
	WDA12-97	39	20	4	5	17	3	12	m-tr	65	35
	WDA12-99	41	19	3	5	17	2	13	m-tr	66	34
Group 1 (n = 13)	Min.	32	18	3	4	13	4	11	--	62	32
	Max.	42	23	4	7	20	7	13	--	68	38
	Average	35.4	21.4	3.4	5.3	17.1	5.1	12.5	tr	65.3	34.8
	SD	2.95	1.65	0.50	0.83	1.86	1.00	0.65	--	1.82	1.82
	Median	34.5	21.5	3	5	17	5	13	--	65	35
Group 2 (n = 26)	Min.	31	18	3	3	17	2	10	--	58	33
	Max.	39	21	4	7	25	8	16	--	67	42
	Average	34.6	19.0	3.0	4.7	19.1	5.7	13.9	tr	61.3	38.7
	SD	1.82	0.73	0.19	0.91	1.63	1.11	1.25	--	1.75	1.75
	Median	34	19	3	5	19	6	14	--	61	39
Group 3 (n = 9)	Min.	32	18	3	4	11	5	11	--	59	29
	Max.	43	21	4	6	21	11	15	--	71	41
	Average	35.7	19.5	3.1	4.9	17.1	6.9	12.8	tr	63.2	36.8
	SD	3.33	1.08	0.32	0.57	3.28	1.60	1.32	--	3.77	3.77
	Median	35.5	19.5	3	5	18	7	13	--	62.5	37.5

Hence, for these two samples, the results can be considered semiquantitative. Furthermore, the variation in mineral content for each group is minimal. The clay minerals, in decreasing abundance are muscovite, chlorite, and kaolinite. Samples WDA12-97 and WDA12-99 have nonclay contents of 65% and 66, respectively, comparable to all three sediment groups.

### Sediment texture

Polished thin sections were used to examine the sediment texture of samples WDA12-97 and WDA12-99; high-resolution scans of the sections are shown in Figure 5. The clay samples show a massive clay structure with irregularly distributed silt lenses throughout both samples. Cracks are due to the impregnation technique and polishing processes and do not reflect structural changes.

Detailed SEM photomicrographs are shown in Figures 6 and 7. As noted above, silt lenses were observed within the massive fine-grained materials in both samples. These lenses consist of poorly sorted grains within a mica-rich clay-size matrix. The minerals were subangular to subrounded and primarily composed of quartz, feldspar, chlorite, and mica. Trace minerals such as rutile, apatite, and Fe-oxide minerals were also noted. In addition, a single pyrite framboid was observed within WDA12-99 (Fig. 7c).

## DISCUSSION

### Physical properties

#### Grain size

Based on the grain-size analysis, the samples may be classified into three distinct categories: fine-grained Group 1 sediments underlying silty Group 2 sediments, with an upper sandy, Group 3 layer. From these stratigraphic groupings, it

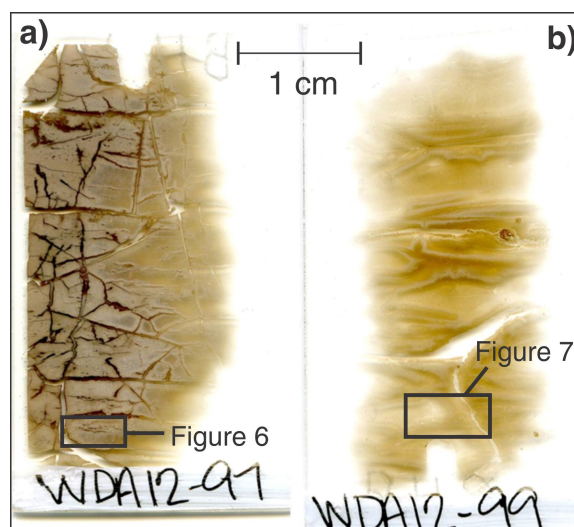


**Figure 5.** Polished thin sections of clay samples a) WDA12-97 (2015-083) and b) WDA12-99 (2015-092).

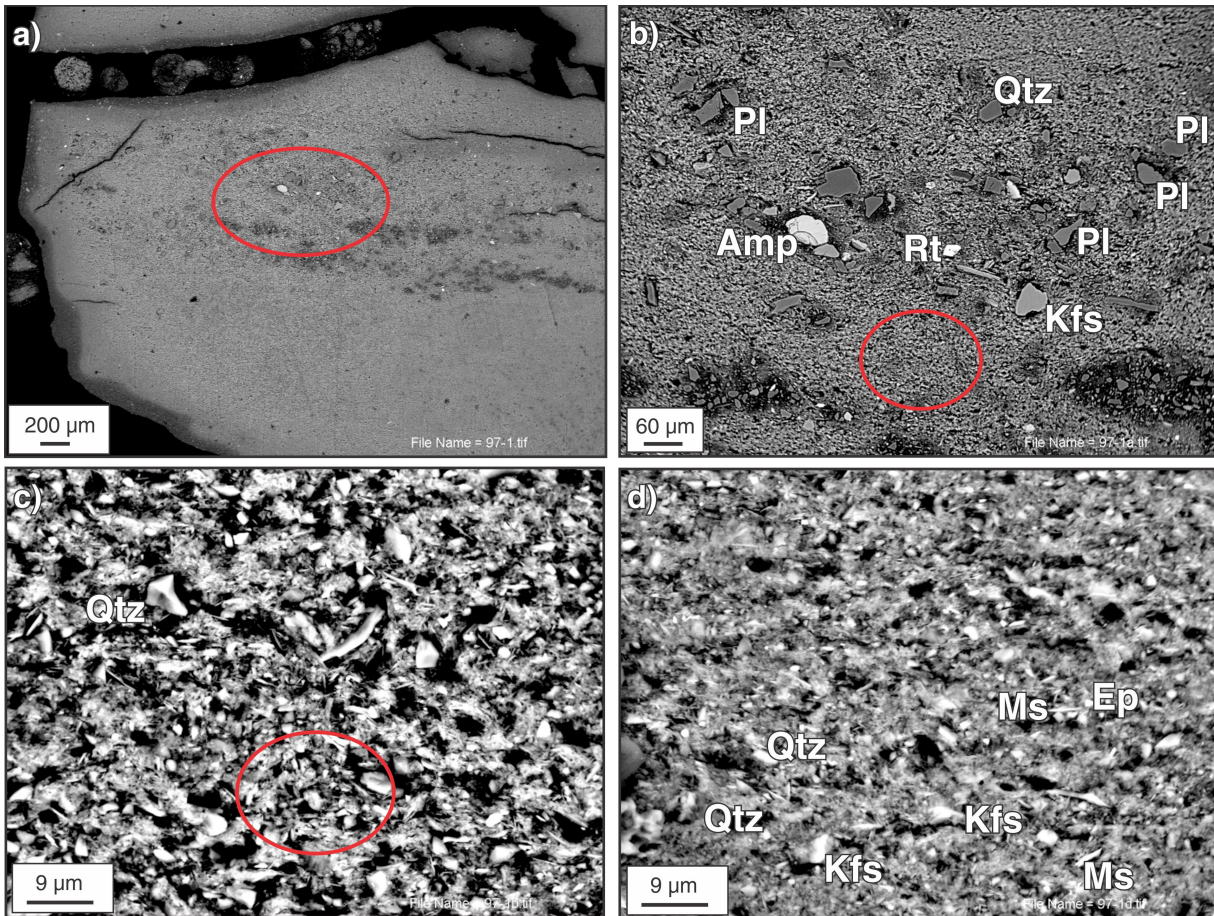


**Figure 6.** Scanning electron microscope photomicrograph backscattered image of: **a)** silt lenses within WDA12-97 clay sample; 2015-090; **b)** close-up of circled area in Figure 6a; 2015-093; **c)** close-up of circled area in Figure 6b; 2015-086; **d)** focus on circled area in Figure 6c (same scale); 2015-095. Amp = amphibole, Ep = epidote, Kfs = potassium feldspar, Ms = muscovite, PI = plagioclase feldspar, Qtz = quartz, Rt = rutile

is interpreted that the Group 1 sediments most probably represent deep-water deposits of glacial Lake McConnell, whereas the coarser grained Group 2 and Group 3 sediments constitute shallow-water lacustrine or alluvial deposits of ancestral Great Slave Lake (Kerr and Wilson, 2000). Dropstones, which are comparatively large-sized clasts found within fine-grained sediments, typical of glaciolacustrine environments (Bennett et al., 1996), were found within Group 1 sediments.

### Atterberg limits

All Group 1 samples reside above the A-line (Fig. 4c). Samples WDA12-97 and WDA12-99 are characterized as inorganic clays with high plasticity (Holtz and Kovacs, 1981) and are classified as inactive. Activity is a parameter defining the extent to which the clay fraction has an impact on the Atterberg limit properties of the soil and how vulnerable these soils are to any changes in these properties (Mitchell,

1976). It can also be used to determine the dominant clay type within the soil. Based on these results, the dominant clay type is nonswelling (Mitchell, 1976).

### Moisture content and bulk density

Group 1 samples contain relatively high moisture contents (Table 1). This represents the volumetric increase in ice lenses with increasing depth, with the largest volume found in the lowermost clay unit (Fig. 3). Furthermore, based on the frozen bulk-density values, the soil samples appear to be stiff and consolidated. This suggests that during the freezing process, consolidation of these samples has occurred as water migrated to the freezing plane to form the ice lenses (Chamberlain, 1981). Fall cone tests conducted on samples WDA12-97 and WDA12-99 further confirmed that consolidation of these samples has occurred.

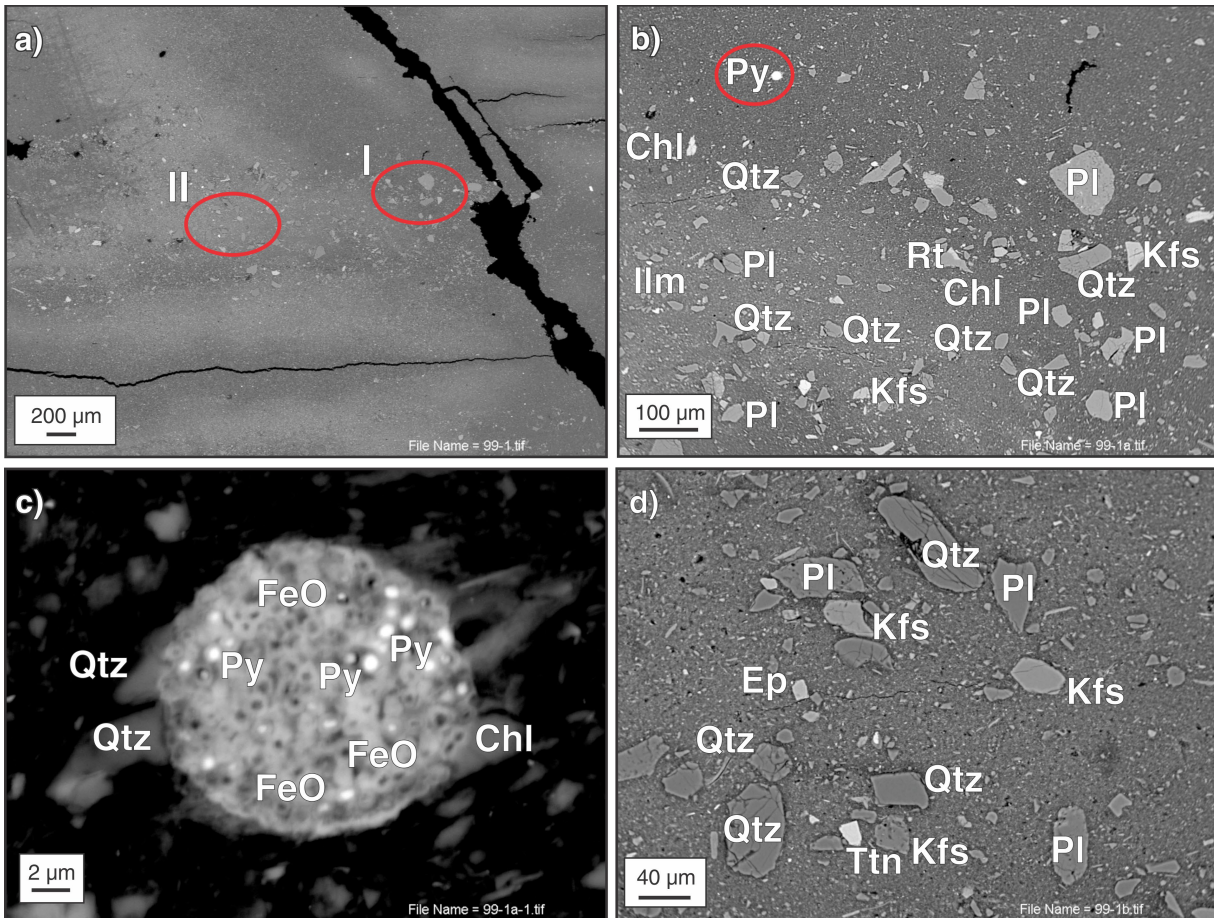


**Figure 7.** Scanning electron microscope photomicrograph backscattered image of: **a)** silt lenses in WDA12-99 sample; 2015-091; **b)** close-up image of circled area I in Figure 7a; 2015-084; **c)** close-up of pyrite framboid embedded with Fe-oxide grains found within Figure 7b; 2015-088; **d)** close-up image of circled area II in Figure 7a; 2015-085. Chl = Chlorite; Ep = epidote; FeO = iron oxide; Kfs = potassium-feldspar, Ilm = ilmenite, Pl = plagioclase feldspar, Py = pyrite (framboid), Qtz = quartz, Rt = Rutile, Ttn = titanite

## Mineralogy

Within the bulk (<2 mm) fraction, quartz and feldspar contents vary among the sediment groups, with quartz increasing significantly from Group 1 to Group 3 as grain size increases. In contrast, amphibole and K-feldspar amounts decrease, as do the proportions of clay minerals. The mineralogy of the clay-size fraction appears to be similar among the sediment groups. This implies that all of the sediments have the same source, and variation reflects the difference in grain-size distribution.

The clay mineralogy is comprised primarily of detrital mica (i.e. muscovite), chlorite, and kaolinite, with trace mixed-layer clay minerals (probably illite-smectite). Previous studies have examined the possibility of chemical weathering to explain the origins of mica and chlorite minerals in glacially derived sediments; however, glacial transport results in intense physical weathering and running glacial water cannot be the sole cause of observable mineral changes (Chamley, 1989). Thus, the occurrence of clay

minerals in these environments is due primarily to physical processes (Chamley, 1989). The large quantity of mica and chlorite indicate that the parent materials are derived from igneous or metamorphic bedrock. The plutonic granite, granodiorite, and tonalite rocks found locally are the most likely source; however, the presence of mixed-layer clay minerals, which typically originate from alteration of previously existing clay minerals such as during weathering (Środoń, 1999), indicate that some chemical weathering could have occurred. According to Chamley (1989), the presence of clay minerals along with rare mixed-layer clay minerals are essentially detrital and derive from reworking of local bedrock sources.

Although the authors ascertain that these sediments are derived locally, is it possible they originated from glacial Lake Agassiz? There are at least two northern outflows of this large glacial lake into the Mackenzie River (ca. 12.9–9.5 ka) that have been mapped (Thorleifson, 1996); however, mineralogical composition of Lake Agassiz materials show the

existence of carbonate minerals (Thorleifson, 1996), which were not detected in the samples in this study. The minerals found in this study, however, are more comparable to those found in the Champlain Sea sediments in the Ottawa River–St. Lawrence River valleys region. These materials, i.e. Leda clay, contain glacially ground detrital material derived from the local Precambrian bedrock (Percival et al., 2003).

The younger deposited sediments containing only trace amounts of mixed-layer clay minerals may be due to further reworking of the Group 1 sediments and greater mixing with local sediment sources (i.e. Great Slave Lake). The plasticity, as well as the normal activity to inactivity indicated by the Atterberg limits, is most likely due to the presence of the clay minerals (Mitchell, 1976). In addition, the overall similarity in the clay-fraction composition among the three groups generally suggests a common origin.

### Sediment texture

Clay fabric is defined as the geometric arrangement of individual minerals within a clay matrix and is a significant parameter for assessing overall soil structure (Yong and Warkentin, 1975). From the detailed SEM analysis, the two samples examined are massive clay with randomly distributed silt lenses. These silt lenses are composed of detrital minerals such as quartz, feldspar, amphibole, and traces of zircon and iron-oxide minerals. The silt particles themselves are angular to subrounded and are supported by the clay matrix.

A pyrite framboid was found in WDA12-99, with Fe-oxide particles embedded within the particle. This suggests a reducing environment with anaerobic conditions (Percival et al., 2003). Although the origin is unknown, the ‘framboid’ may simply represent organic matter that was altered in situ. Pyrite is a common alteration mineral product of organic matter during early diagenesis (Taylor and Macquaker, 2000). Thus, a likely explanation for the formation of the ‘framboid’ is related to development of anaerobic conditions in deeper sediments. Indeed, the hydrological properties of clay-rich sediments can provide the means for a saturated and reducing environment for organic matter to become altered to pyrite.

Lamination is common in glacial environments and maybe indicative of glaciolacustrine origins (O’Brien and Pietraszek-Mattner, 1998). Although only two thin sections were examined for the purpose of this study, based on the detailed SEM analysis, the clay microfabric observed indicates minimal lamination throughout the entire clay unit.

Nevertheless, a question remains as to the origins of the silt lenses within the massive clay matrix. When analyzing the microfabric of glaciolacustrine sediments to infer depositional processes, O’Brien and Pietraszek-Mattner (1998) determined, through SEM analysis, that the most influential depositional mechanism was most likely slow settling of suspended matter. A high concentration of suspended matter

would lead to the suspended particles flocculating together due to electrochemical attraction (O’Brien and Pietraszek-Mattner, 1998); however, in these samples, the silt-rich lenses show individual silt-size grains. Thus, the silt lenses could represent episodic deposition. There is no evidence that these are varved sediments based on the textural study completed, as the layers or laminations do not appear to be demonstrably annual or cyclical. Therefore, these silt lenses more likely reflect the glaciolacustrine origin of these clay sediments.

Lastly, it is interesting to note the orientation among the grains. All of the SEM images show random distribution of the coarser grains within the clay matrix; the clay minerals themselves also form a loose microstructure. During incipient diagenesis, the loosely packed clay minerals will orient themselves more densely with an increase in overburden pressure from overlying sediments, a process called compaction. When this occurs, there is a reduction in water content, a decrease in the volume of sediments, which causes change in the microstructure of sediments (Singer and Muller, 1983). Yet, as noted from the detailed SEM analysis, there is a parallel orientation of the phyllosilicate minerals, which may be indicative of minor compaction.

---

## INFRASTRUCTURE IMPLICATIONS

An increasingly challenging problem for infrastructure development in permafrost environments is high ground-ice contents within fine-grained sediments. Common issues faced during construction are thaw subsidence and frost heaving (French, 2007). This is particularly noted in areas such as Yellowknife, where discontinuous permafrost is associated with unconsolidated materials that, due to their hydraulic properties, contain significant proportions of excess ice (French, 2007; Wolfe et al., 2014). The presence of ice-rich permafrost within glaciolacustrine and lacustrine sediments in the Great Slave Lowland implies that these areas are indeed thaw-sensitive, and any infrastructure built upon this terrain will settle if the permafrost thaws. This has occurred on Highway 3, where ice-rich permafrost thaw resulted in settlement of the embankment due to highway construction (Wolfe et al., 2014). For this, it is critical to understand the geotechnical and mineralogical nature of the ground where infrastructure developments are proposed.

---

## CONCLUSIONS

The objective of this study was to analyze the geotechnical, mineralogical, and textural properties of two clay-rich samples, WDA12-97 and WDA12-99, and to compare these results to other samples collected in the area as part of a larger study to understand permafrost conditions and the existence of ice-rich terrain. From the physical property analysis of the larger population of samples, three distinct groupings

were determined based on grain-size distributions: clay-rich (Group 1), silt-rich (Group 2), and silty-sand-rich (Group 3). The two selected samples fall within Group 1. These samples are glaciolacustrine in origin, derived from glacial Lake McConnell. Samples WDA12-97 and WDA12-99 lie above the A-line of the Casagrande plot, characterizing them as inorganic clay with medium to high plasticity. Other Atterberg limit results show that these samples are also inactive. Mineralogy results show that the nonclay minerals include quartz, feldspar, and amphibole. The main clay minerals are mica, chlorite, and kaolinite, with traces of mixed-layer clay minerals. Within the bulk fraction, there is a large variation between mineral contents among the groups; however, less variation exists within the clay-size fraction. Evidence suggests that the younger deposited sediments are reworked Group 1 sediments. The SEM analysis shows that WDA12-97 and WDA12-99 are massive clay with randomly distributed silt lenses composed of detrital minerals (e.g. feldspar, amphibole, and traces of zircon and Fe-oxide minerals). The high volumes of ice within the ground may result in unstable ground.

---

## ACKNOWLEDGMENTS

The authors would like to thank P. Hunt for SEM analysis and I. Jonasson for sample impregnation. A. Gaanderse and P. Morse are acknowledged for collecting the samples, and P. Morse for his critical review of this manuscript.

---

## REFERENCES

- Arctic Climate Impact Assessment, 2005. Arctic Climate Impact Assessment; Cambridge University Press, Cambridge, United Kingdom, 1042 p.
- Bennett, M.R., Doyle, P., and Mather, A.E., 1996. Dropstones: their origin and significance; *Palaeogeography, Palaeoclimatology, Palaeoecology*, v. 121, p. 331–339. [doi:10.1016/0031-0182\(95\)00071-2](https://doi.org/10.1016/0031-0182(95)00071-2)
- Burn, C.R. and Smith, M.W., 1993. Issues in Canadian permafrost; *Progress in Physical Geography*, v. 17, p. 156–172. [doi:10.1177/030913339301700204](https://doi.org/10.1177/030913339301700204)
- Burn, C.R., Barrow, E., and Bonsal, B., 2004. Climate change scenarios for Mackenzie River valley; 57<sup>th</sup> Canadian Geotechnical Conference and the 5<sup>th</sup> Joint Canadian Geotechnical Society–International Association of Hydrogeologists Conference, Quebec, p. 24–27.
- Chamberlain, E.J., 1981. Overconsolidation effects of ground freezing; *Engineering Geology*, v. 18, p. 97–110. [doi:10.1016/0013-7952\(81\)90050-8](https://doi.org/10.1016/0013-7952(81)90050-8)
- Chamley, H., 1989. *Clay Sedimentology*; Springer-Verlag, New York, New York; Berlin, Germany, 623 p. [doi:10.1007/978-3-642-85916-8](https://doi.org/10.1007/978-3-642-85916-8)
- French, H.M., 2007. *The Periglacial Environment*; John Wiley & Sons, Hoboken, New Jersey, Chichester, England, 458 p. (third edition). [doi:10.1002/9781118684931](https://doi.org/10.1002/9781118684931)
- Girard, I., Klassen, R.A., and Laframboise, R.R., 2004. *Sedimentology laboratory manual*, Terrain Sciences Division; Geological Survey of Canada, Open File 4823, 134 p. [doi:10.4095/216141](https://doi.org/10.4095/216141)
- Holtz, R.D. and Kovacs, W.D., 1981. *An Introduction to Geotechnical Engineering*; Prentice-Hall, Englewood Cliffs, New Jersey, 733 p.
- Kerr, D.E. and Wilson, P., 2000. Preliminary surficial geology studies and mineral exploration considerations in the Yellowknife area, Northwest Territories; *Geological Survey of Canada, Current Research 2000-C3*, 8 p. [doi:10.4095/211101](https://doi.org/10.4095/211101)
- Maxwell, B., 1997. Responding to global climate change in Canada's arctic; *in* Volume II of the Canada Country Study: Climate Impacts and Adaptation; Environment Canada, Toronto, Ontario, 82 p.
- Mitchell, J.K., 1976. *Fundamentals of Soil Behavior*; John Wiley & Sons, New York, New York, 449 p.
- O'Brien, N.R. and Pietraszek-Mattner, S., 1998. Origin of the fabric of laminated fine-grained glaciolacustrine deposits; *Journal of Sedimentary Research*, v. 68, p. 832–840. [doi:10.2110/jsr.68.832](https://doi.org/10.2110/jsr.68.832)
- Percival, J.B., Hunt, P., and Wyergangs, M., 2001. Mineralogical investigations of Canadian till and lake- and-stream sediment reference materials: part 1. Standardized X-ray diffraction and scanning electron microscope methods; *Geological Survey of Canada, Current Research 2001-E9*, 20 p.
- Percival, J.B., Aylesworth, J., and Fritz, A., 2003. Analysis of colour rhythmites in sensitive marine clays (Leda clay) from Eastern Canada; *in* 2001: A Clay Odyssey. (ed.) E.A. Domingues, G.R. Mas, and F. Cravero; *Proceedings, 12<sup>th</sup> International Clay Conference, Bahia Blanca, Argentina, July 22–28, 2001*, p. 147–154.
- Percival, J.B., Wolfe, S.A., and Grenier, A., 2013. Origin of lacustrine clays in the Great Slave Lowlands, Northwest Territories, Canada and implications for terrain stability; *XV International Clay Conference, July 2013, Rio de Janeiro, Brazil* (abstract).
- Singer, A. and Muller, G., 1983. Diagenesis in argillaceous sediments; *in* Diagenesis in Sediments and Sedimentary Rocks 2, (ed.) G. Larsen and G.V. Chilingar; Elsevier Scientific Publishing Company, Amsterdam, The Netherlands; New York, New York, p. 115–212.
- Środoń, J., 1999. Nature of mixed-layer clays and mechanisms of their formation and alteration; *Annual Review of Earth and Planetary Sciences*, v. 27, p. 19–53. [doi:10.1146/annurev.earth.27.1.19](https://doi.org/10.1146/annurev.earth.27.1.19)
- Stevens, C.W., Kerr, D.K., Wolfe, S.A., and Eagles, S., 2012a. Predictive surficial material and geology derived from LANDSAT 7, Yellowknife, NTS 85J, Northwest Territories; *Geological Survey of Canada, Open File 7108*, 31 p. [doi:10.4095/291731](https://doi.org/10.4095/291731)
- Stevens, C.W., Wolfe, S.A., and Gaanderse, A.J.R., 2012b. Lithals distribution, morphology and landscape associations in the Great Slave Lowlands, Northwest Territories; *Geological Survey of Canada, Open File 7255*, 41 p. [doi:10.4095/292115](https://doi.org/10.4095/292115)

- Taylor, K.G. and Macquaker, J.H.S., 2000. Early diagenetic pyrite morphology in a mudstone-dominated succession: the Lower Jurassic Cleveland Ironstone Formation, eastern England; *Sedimentary Geology*, v. 131, p. 77–86. [doi:10.1016/S0037-0738\(00\)00002-6](https://doi.org/10.1016/S0037-0738(00)00002-6)
- Thorleifson, L.H., 1996. Review of Lake Agassiz history; *in* *Sedimentology, Geomorphology, and History of the Central Lake Agassiz Basin*, (ed.) J.T. Teller, L.H. Thorleifson, G. Matile, and W.C. Brisbin; Geological Association of Canada, Field Trip Guidebook B2, p. 55–84.
- Wolfe, S.A., Duchesne, C., Gaanderse, A., Houben, A.J., D’Onofrio, R.E., Kokelj, S.V., and Stevens, C.W., 2011. Report on 2010–2011 permafrost investigations in the Yellowknife area, Northwest Territories; Geological Survey of Canada, Open File 6983, 75 p., 1 CD-ROM. [doi:10.4095/289596](https://doi.org/10.4095/289596)
- Wolfe, S.A., Stephens, C.W., Gaanderse, A.J., and Oldenborger, G.A., 2014. Lithals distribution, morphology and landscape associations in the Great Slave Lowland, Northwest Territories, Canada; *Geomorphology*, v. 204, p. 302–313. [doi:10.1016/j.geomorph.2013.08.014](https://doi.org/10.1016/j.geomorph.2013.08.014)
- Yong, R.N. and Warkentin, B.P., 1975. *Soil Properties and Behavior*; Elsevier Scientific, Amsterdam, The Netherlands, 449 p.

---

Geological Survey of Canada Project 343202NP21